SASEC
1st Southern African Solar Energy Conference
21-23 May 2012

CONTROL DESIGN PROFITS HELIOSTAT TECHNO-ECONOMICS

Nick Rubin[1], Thomas Roos[2], Fintan Wilson[2], Jason de Villiers[2] and Srinivasan Perumal[2]

1 Systems Engineer – CSIR, P O Box 395, Pretoria, 0001, South Africa, Phone: 0128413383, Fax:0128413179, NRubin@csir.co.za 2 THRoos@csir.co.za, FWilson@csir.co.za, JdVilliers@csir.co.za, SPerumal@csir.co.za

Abstract

Modelling, Identification, Simulation and Synthesis are well known components of the System Engineering Process. Ally these with the Target Aligned (TA) heliostat architecture and the universally acknowledged merits of using closed loop feedback control, then one has all the requisite tools to produce a cost effective solar energy product that can deliver impact in the renewable energy arena.

Keywords: Heliostat; CSP field; two axis control; cost-benefit tradeoff

1. Introduction

Roos [1] motivates that the use of heliostat reflectors for solar power concentration, combined with the conversion of thermal to electrical energy via a gas turbine, is economically attractive for remote, semi-rural settlements. For reasons of reducing complexity and cost, theoretically desirable, spheroidal mirror profiles are often realized using facetted mirror panels. Unless the sections are specifically and uniquely formed to be part of the original spheroid, the individual sections must be canted inwards to form a tight image on the collector plane. Such canting is only accurate for one particular solar elevation and azimuth, at all other incidence angles, aberration defocuses the composite spot from the individual images. As motivated by Ries et al. [2], Target Aligned (TA) heliostats have the promise of improving power efficiency due to reducing these aberration effects, since the solar incidence angle at the mirror is constrained to lie in the sagittal (pitch) plane of the mirror. On long summer days, Chen et al. [3] estimate the reduction in spillage at the receiver, using TA heliostats, to be between 10 % and 30 % (dependent on receiver area).

This paper reports on the improvements in tracking performance, and the economic impacts associated with reduced spillage at the receiver, that accrue through analysis, modelling and control design techniques.

2. Background

2.1. Previous Results

The CSIR performs experimental work using two target aligned heliostats : a 1,25 m^2 experimental heliostat [4] and a prototype 25 m^2 heliostat [5]. Both heliostat position control systems use rotary actuation around the high inertia, roll axis, and linear actuation in pitch, and an optical tracker as the attitude sensing device.

A custom-built, two-axis controller was initially developed for the smaller heliostat, which was developed as a joint project with the University of Natal, SA, in 2007. This controller used simple, independent, bang-bang control of the pitch and roll axes, for which a worst case image positioning error of 3,3 mrad was achieved [1]. This controller was thereafter modified to also control the significantly higher inertia, 25 m^2 heliostat. The effective proportional gain of these two loops was, in both cases, found by trial and error by simply reducing gain to back off from the point of instability. This design architecture, and controller tuning strategy, provided fairly tight tracking performance for high solar elevation angles, although it was susceptible to limit-cycling (amplitude constrained instability) when the sun was far from zenith.

It is testimony to the robustness of feedback control that a purely stabilizing tuning of two independent controllers, at the nominal operating point, resulted in respectable tracking performance of the coupled positioning system over most of the operational envelope. However stabilisation is merely a necessary attribute of a good control system, further requirements typically also include acceptable regulation performance and disturbance rejection.

3. Design Considerations and Technical Performance

3.1. Updated Controller Design

A controller hardware change was necessitated due to the custom designed hardware, built with the 2007 vintage experimental heliostat, being unmaintainable. Accordingly a COTS, two-axis controller module was acquired, which includes dual integrated H-bridge servo drives and over-current and thermal protection. Furthermore, the upgraded control algorithm was explicitly designed to address actuator backlash, and was implemented using dual control strategies that operate in parallel. The first strategy implements a simple, and so robust, proportional control with significant low pass filtering, to realise good steady state regulation.
The second strategy incorporates a model reference controller which acts to prevent the deleterious effects of backlash. Significant filtering of the optical tracker signals was performed, including a sharp notch filter at 50 Hz. The controller cyclic rate was 180 actuations per second, while the ARM core powering the controller has the capability to clock the digital filters at 14 000 samples per second.

Bang-bang actuation commands are once again generated, even though the COTS controller does provide PWM modulation, potentially yielding finer control. This strategy was retained for compatibility with local-content motor control modules that are already under development at the CSIR for robotic applications.

3.2. Test Method

Performance was characterised in tests during 2011 (of the original controller) and 2012 (for the updated controller). The test modus operandi was identical in both cases. The heliostat was oriented to reflect the solar image over a nominal range of 59 m onto the vertical wall of a building, close to perpendicular with respect to the heliostat attitude (see Fig. 1). All but a single mirror facet were masked, to cast a close to circular image. Step, ramp and normal solar tracking tests were performed and recorded by video camera from an average slant range of 12 m. The wall used as the projection surface comprised rectangular blocks, which provided a natural fiduciary grid, which was surveyed using a laser range finder. The local earth co-ordinates of critical blocks were deduced from the range data.

Where the tests did vary was in the actual video equipment used and the method of analysis. The 2011 tests benefitted from the assistance of the Image Processing group at CSIR Optronics. The dynamic image motion was recorded at 20 fps with a 1600x1200 pixel, Prosilica GE1660 video camera using a 5 mm, f1,4 lens to give an 82° azimuth field of view, but with associated, significant lens distortion.

The 2012 tests were recorded at 28 fps with a 640x480 pixel, Pentax E30, digital camera using a 6-18 mm, f2,7-f4,8 lens, zoomed to an 18.5° azimuth field of view. This camera's image integrity had previously been tested and found to have acceptably low distortion of straight horizontal and vertical lines, and is believed to have sufficient internal lens correction.

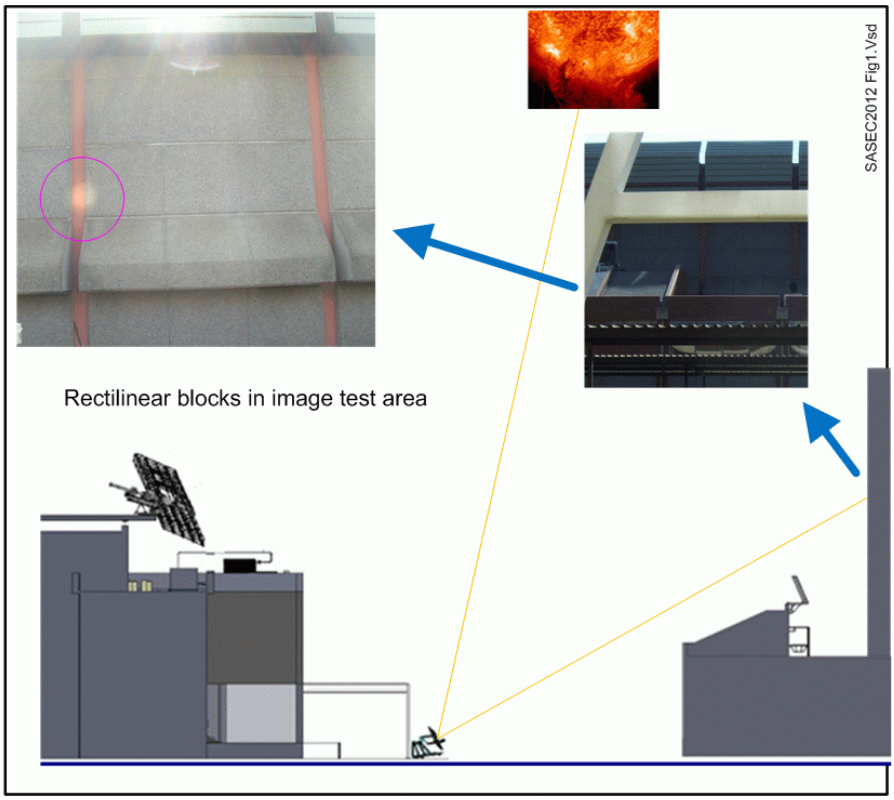

Fig. 1. Heliostat Test Setup

3.3. Results - Original (2007) Controller

The method of wide angle distortion correction used is described extensively in de Villiers et al. [6], suffice it to say here that the primary requirement in this application was to select an appropriate lens calibration method such that straight lines in the real-world project into straight lines in image space. This correction method was evaluated using regular figures prior to processing the recorded data, with impressive results :

Pattern type	Measurement method	Initial distortion (pixels RMS)	Optimal distortion (pixels RMS)
Open CV Calibration[1]		-	0.770
Circle, size 10	Centroid	347.645	0.081
	Ellipse	347.785	0.088
Circle, size 25	Centroid	335.622	0.078
	Ellipse	335.510	0.142

Table. 1. Image Distortion Correction - Results

The image motion was determined after processing each frame as follows. The frame was de-warped as above and the solar image on the wall was extracted using a threshold filter. The centroid's coordinates in the camera reference frame were determined, as well as the centroid quality measure (related to the number of points detected). The elevation and azimuth coordinates of the centroid, in the camera reference frame, were determined using the survey data of the fiduciary points on the wall, and the time-stamped elevation and azimuth attitude, and centroid quality were output for every frame.

These two attitudes were transformed to angles in the frame centred on the heliostat optical centre, using the earth locations of the camera and heliostat, and appropriate spherical → cartesian, translation and cartesian → spherical operations.

The principal measure of performance chosen was the rms deviation of the image's centroid from its mean position during the test. For interest, the rms values of the individual elevation and azimuth deviations, as well as the pythagorean combination of the two deviations $\sqrt{,\sigma^2(\text{elev}) + \sigma^2(\text{azim})}$, is also presented – as this form of pythagorean combination was assumed by the analysis tool used by DLR [7], which is discussed further in Sec. 4 in the context of economic implications.

The results using the original controller are as follows :

RMS total deviation : σ(total) = 0,55 mrad

RMS elevation deviation : σ(elev) = 0,40 mrad RMS azimuth deviation : σ(azim) = 0,41 mrad

RMS combined deviation : σ(combined) = 0,57 mrad

Figure 2 indicates the time history of the total angular error (red), elevation error (green), azimuth error (blue) and the quality measure (cyan - note this signal's scale factor and offset). The results beyond 325 s correspond to partial cloud obscuration and were ignored in the error calculations.

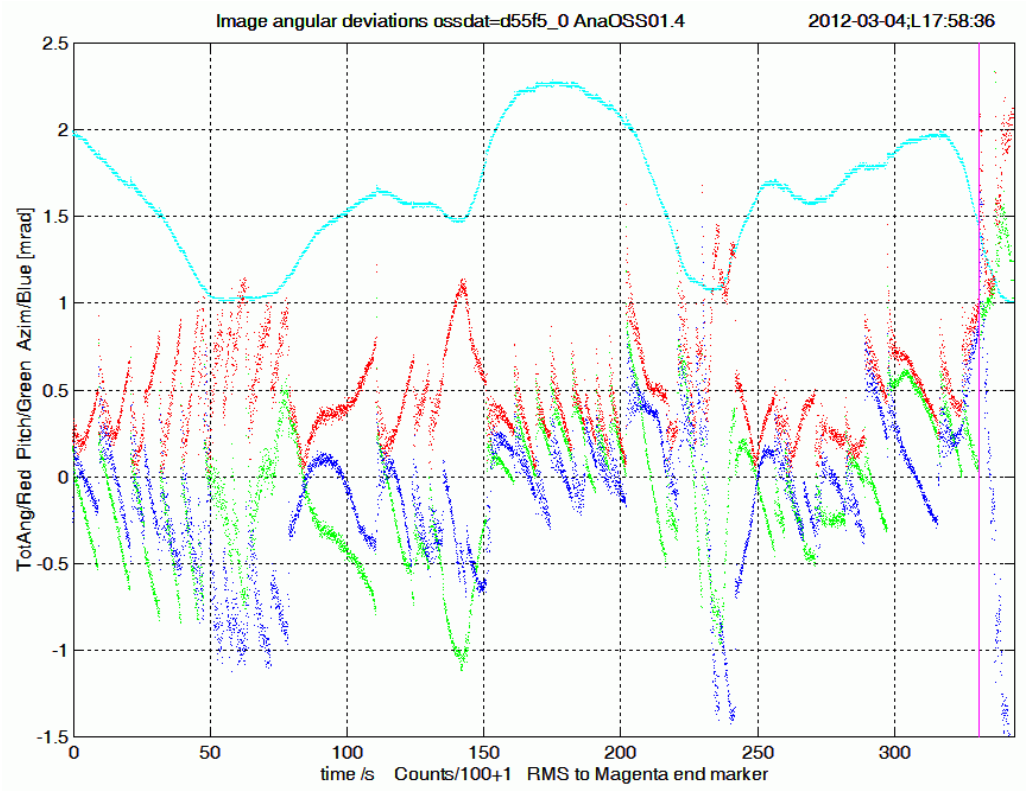

Fig. 2. Angular error deviations for Original Controller

3.4. Results – Updated (2012) Controller

As indicated in Sec. 3.2, no distortion correction was performed and the image motion was determined by visual inspection of each frame. Selected frames at the error extremes were overlayed with measurement outlines to determine the centroid of the solar image and the image scale of fiduciary points in the image. The image coordinates of these outlines were measured off screen and the true location of the solar image centre on the projection surface was calculated directly. Thereafter the same translation and cartesian → spherical transformation were used, as before.

The results using the updated controller are as follows :

RMS total deviation : σ(total) = 0,26 mrad

RMS elevation deviation : σ(elev) = 0,14 mrad RMS azimuth deviation : σ(azim) = 0,23 mrad

RMS combined deviation : σ(combined) = 0,26 mrad

Figure 3 indicates the time history of the elevation error (red) and azimuth error (green). With these results, the total angular error is dominated by the azimuth error and so is not shown. The + symbols (blue) indicate the number of frames which the controller was active correcting accumulated error (note this signal's negative scale factor and offset).

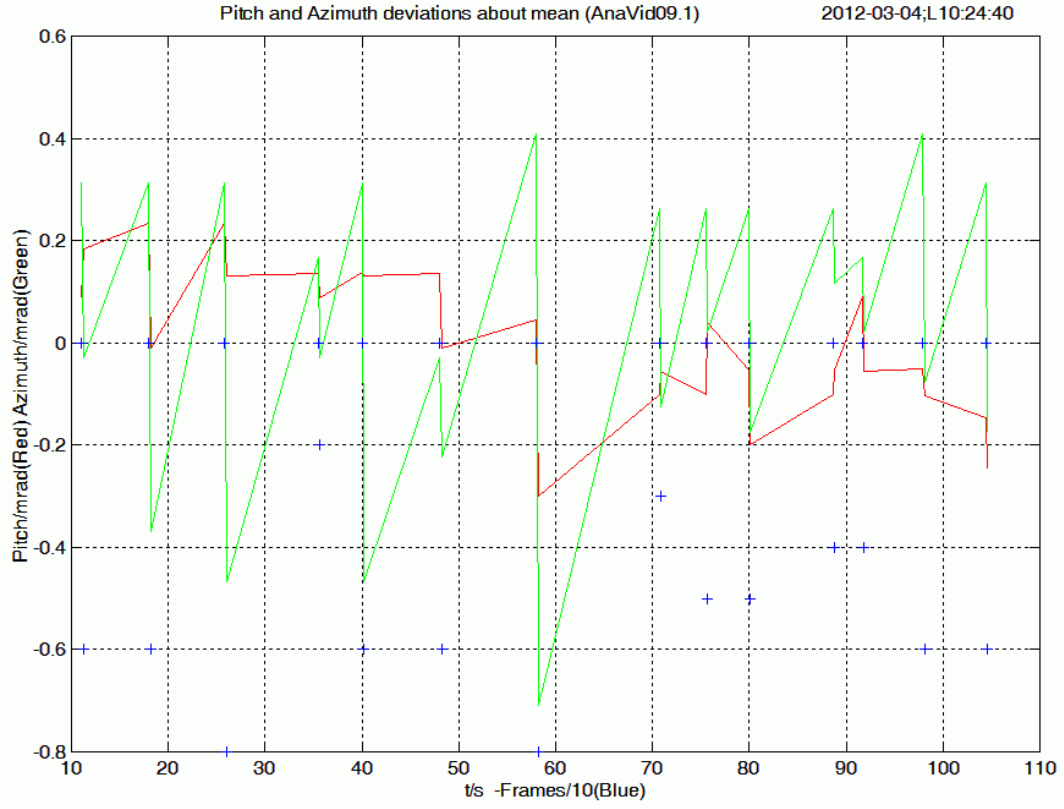

Fig. 3. Angular error deviations for Updated Controller

3.5. Comparison of Controller Performance

A notable result is that the updated controller has reduced the rms of the total angular error deviation, for the specific test conducted, from 0,57 mrad to 0,26 mrad. The economic impact of this on field capital cost is examined below. The nature of the controller responses is also different. The errors with the original controller indicate slower natural frequencies than with the updated controller, which will probably translate into more sluggish disturbance rejection. In contrast, the responses with the updated controller indicate that the controller changes the sign of the error (around the mean) on average every eight seconds, which will probably mean that with wind or other disturbances it will have superior performance.

4. Economic Impact

4.1. Techno-Economic Modelling

This study was performed using the parameters for a field of 13,4 m^2 TA heliostats, which the CSIR proposes in the Solar Power Research Project in order to develop CSP technologies supporting power conversion, thermal storage and secondary power utilisation. DLR performed preliminary field layouts for the CSIR site, initially using their analysis and design tool HFLCAL [7], and these results are used in this study (DLR subsequently refined the layout using ray tracing considerations). One of the principal inputs to HFLCAL is the rms tracking error of the heliostat controller. We examine the cost benefit of improvements in this rms error, using two cases motivated by the level of improvement observed with the 1,25 m^2 experimental heliostat above.

A cost-analysis model had recently been developed at the CSIR to perform a cost-benefit trade-off, in order to form groups of heliostats with identical mirror focal lengths. This model was adapted in order to determine the cost reduction associated with improved tracking performance. However a key assumption made for focal length selection was retained – being that the heliostats are arranged in patterns lying along arcs (rows) in plan view, with these arcs equidistant from the receiver. The layouts from HFLCAL generally have the attribute of equispaced radially and azimuthally heliostat arrangements, to reduce shading and blocking effects, consistent with the arrangement of heliostats along arcs. It is noted that refinements of the layout process, using fine tuning based on ray tracing, perturb the symmetrical pattern, as evidenced in the progression to Figs. 3 and 5 in Buck at al. [7].

The layout in the latter ref's Fig. 3 [7] was generated with assumptions of circular normal distributions for mirror aberrations, control system tracking and solar image spreading. In true aspect ratio this plot indicates the presence of nine constant radius arcs, as well as East-West symmetry. The cost-analysis model lifted the restrictive assumptions of circular normal distributions for all sources of solar image dispersion, and replaced these with normal distributions in elevation and azimuth. Furthermore a more representative (non-normal) solar intensity distribution was used to determine spillage more accurately, and this was superimposed on the centroid position distribution due to mirror surface aberration and control system tracking. Conditions at HFLCAL's design operation point (local noon on the northward equinox) were used and composite power spillage distributions were determined at each radius. These power losses are related to an economic impact by means of calculating the hypothetical, fractional increase in the number of heliostats to return to the power had there been no spillage losses.

4.2. Detailed Causes of Spillage

HFLCAL considers three causes of spillage, indicated below (with the values used for the layout produced) and lumps them into a single parameter, the so called Beam Error [7], but it does not consider canting errors.

Mirror slope rms error, σ(slope) = 1,3 mrad
Tracking rms error, σ(track) = 0,95 mrad
Sun shape rms error, σ(shape) = 2,35 mrad
➔ Beam rms error, σ(total) = 3,99 mrad

Note that the rms values do not combine in a pythagorean fashion, even though statistically uncorrelated effects, since mirror and tracking errors are per axis, and are with reference to the mirror normal and so effectively double in effect in the reflected ray.

HFLCAL uses the beam rms error as the parameter of a zero mean circular normal distribution, assuming that it embodies all of the effects that cause image spread at the receiver. The economic consequence of the spillage resulting from the value used for field layout (3,99 mrad) is compared with what it could be for two scenarios motivated by performance of the upgraded controller.
In the first instance, the effect of nominally halving the controller rms error deviation is considered, motivated by comparing the performance of the 2007 controller with the 2012 upgrade. Secondly, a tracking rms error of 0,95 mrad was provided to DLR, based on expectations of tracking regulator performance, encoder sensor accuracy and disturbances (primarily wind and gravity). However the measured rms error, 0,26 mrad is far lower than this, and it is the total system error for both axes and including all effects on projected image (but noting that gravitational disturbances were small and the wind was light during the tests). If this value is allocated entirely to the control system, this corresponds to setting σ(track) = 0,09 mrad. Below we examine what the economic impact is if that was actually achievable.

4.3. Key results

Table 2 shows the key technical and economic impacts of the different causes of spillage, using the tracking rms error originally provided to DLR (0,95 mrad).

Field Row	Number of heliostats per field row	Total heliostat collection fraction	Total row collection	Total Heliostat cost per row [€]
1	4	1,000	4,000	13931
2	6	1,000	6,000	20897
3	8	1,000	8,000	27863
4	5	1,000	5,000	17414
5	6	1,000	6,000	20897
6	7	1,000	7,000	24380
7	6	0,979	5,875	20897
8	10	0,943	9,432	34829
9	7	0,904	6,327	24380
FIELD TOTAL	59	8,826	57,634	205489
SPILLAGE	**COST**			**€4872**

Table 2. Techno-economic impacts with nominal Tracking Error (0,95 mrad)

The *collection fraction* values indicate the balance after spillage has been modelled, using individual effects in their respective axes. The *total row collection* values incorporate the field layout. The relative shortfall between the total row collection and the value achieved with the total number of heliostats, operating without spillage, is multiplied by the total field cost to obtain the effective economic impact of spillage, in this case nearly 5 000 Euro.

Table 3 shows the effect of tracking performance on the equivalent economic costs of spillage should the tracking error be halved from 0,95 to 0,475 mrad, and then further reduced to the level measured during test (acknowledging that this is still hypothetical performance until full envelope tests have been conducted).

Case	Design Performance	Double Performance	Hypothetical Performance
RMS Tracking Error [mrad]	0,95	0,475	0,09
Image Equiv Tracking Error [mrad]	2,69	1,34	0,26
RMS Beam Error [mrad]	3,99	3,63	3,51
Cost of Spillage [€]	**4872**	**3322**	**2862**

Table 3. Techno-economic impact of tracking performance

Qualitatively it shows the smaller relative effect of decreases significantly below the 0,5 mrad tracking error level. From a cost perspective alone, the law of diminishing returns applies to reducing the tracking error to, what is by all accounts, a dramatically small tracking error of 0,09 mrad. By comparison average human acuity for general perception is around 0,17 mrad, with optimum acuity of 0,002 mrad only being achieved for a single fine dark line against a uniformly illuminated background.
Quantitatively, if the original tracking rms error of 0,95 mrad /axis /mirror_normal tracking error is halved, the equivalent economic benefit on capital outlay is around 1500 Euro (viz. €4872 - €3322) for a 59 heliostat field. Given twice as accurate tracking performance (0,475 mrad rms), the total angular rms deviation of the image relative to the heliostat is a factor of $2\sqrt{,2}$ larger than this, viz. 2,69 mrad, due to a doubling effect by reflection and the combination of independent elevation and azimuth errors. By way of comparison, if a total angular rms deviation of 0,26 mrad were actually achieved, this corresponds to 0,09 mrad /axis /mirror_normal, with a more modest further saving of 460 Euro.

Conclusions

This paper reports on the improvements in image pointing performance of a Target Aligned heliostat that have been realised through an upgraded tracking controller, with a more than 50% reduction in the total system rms tracking error to 0,26 mrad. This improvement has been related to the reduction in economic cost of spillage, with a ballpark figure of 1500 Euro in capital expenditure on a 59 heliostat field. Such impact will scale up according to the size of commercial size CSP fields, so that with a 5 MW_{ELEC} field the potential saving is of the order of fifty times this amount.

Acknowledgements

This work was supported and funded by the Council for Scientific and Industrial Research.

References

[1] Roos, T., et al., 25 m^2 Target-Aligned Heliostat with Closed-Loop Control, SES Solar World Congress 2007: Solar Energy and Human Settlement, Beijing, China, 18-21 September 2007

[2] Ries, H., Schubnell, M., The Optics of a Two-Stage Solar Furnace, Solar Energy Materials, 21 (1990)

[3] Chen, Y., et al., Comparison of Two Sun Tracking Methods in the Application of Heliostat Field, Journal of Solar Energy Engineering 126 (2004)

[4] Maliage, M., Roos, T., The Distribution from a 1,25 m^2 Target Aligned Heliostat: Comparison of Ray Tracing and Experimental Results, submitted to SASEC2012, 21-23 May 2012, Stellenbosch

[5] Roos T., Buck R., Pfahl A., Design of a Multi-Purpose Target-Aligned Heliostat Field, Proceedings ISES SWC 2009, 11-14 October 2009, Johannesburg

[6] de Villiers, J., Wilson, F., Nicolls, F., The effects of Lens Distortion Calibration Patterns on the Accuracy of Monocular 3D Measurements, PRASA2011, Proc. 22nd Ann. Symp. Pattern Recognition Soc. SA

[7] Buck, R., Pfahl, A., Roos, T., Target Aligned Heliostat Field Layout for Non-Flat Terrain, submitted to SASEC2012, 21-23 May 2012, Stellenbosch